Journal of Engineering Mechanics and Machinery (2026)
Clausius Scientific Press, Canada

DOI: 10.23977/jemm.2026.110205
ISSN 2371-9133 Vol. 11 Num. 2

Effects of Seat Rotation Angle on Occupant Head–Neck Injury Responses in Rear Impact

Tingwei Feng, Shihai Cui*

School of Mechanical Engineering, Tianjin University of Science and Technology, Tianjin, China

Keywords: Rear Impact, Seat Rotation Angle, Biomechanical Human Body Model, Neck Injury, Head Injury

Abstract: To address the novel occupant posture safety issues associated with rotating seats in intelligent driving scenarios, rear-impact simulations were conducted using the THUMS AM50 human model under four seat angles (0 °, 45 °, 90 ° and 135 °). By evaluating neck injury criteria (Nkm and NIC), brain injury criterion (BrIC), cervical spine segmental loads, and brain tissue strain responses, the influence of seat rotation on head–neck injury mechanisms was thoroughly investigated. The results indicate that the segmental Nkm response remains relatively low under the standard 0 ° upright posture. In contrast, rotated seating postures induce relative motion between the head and neck, leading to generally elevated levels of segmental Nkm, NIC, BrIC, and brain strain compared to the baseline condition. Notably, a prominent local rotational risk appears at the C7–T1 segment in the 135 ° case. This study reveals the potential head–neck injury risks of rotating seats in rear impacts and provides quantitative data to support safety assessments of intelligent vehicle.

1. Introduction

The development of intelligent driving technologies is changing the role and activities of vehicle occupants [1]. In highly automated vehicles or intelligent cabins, occupants may shift from conventional drivers to participants in in-vehicle activities such as reading, working, resting, or communication [2]. Compared with fixed forward-facing seats, rotating seats, lateral seating postures, and large-angle occupant orientations are more likely to occur, which challenges occupant protection systems developed mainly for standard seating postures [3-4].

Rear impact is one of the important crash scenarios associated with occupant head and neck injuries [5]. Under a standard forward-facing posture, the head–neck response is mainly characterized by a typical whiplash motion. However, under rotated seating postures, the initial occupant orientation, torso loading direction, head restraint contact timing, and cervical segmental load transfer path may all change. As a result, existing rear-impact evaluation methods may not fully reflect local injury risks under non-standard postures [6].

Existing studies have mainly focused on standard seating postures, reclined postures, or restraint system parameters. The head–neck injury mechanism caused by seat angle variation in intelligent driving scenarios remains insufficiently understood. In particular, for a 50th percentile male occupant under a 0 °standard posture and typical rotated postures of 45 °, 90 °, and 135 °, the effects of seat angle on neck injury indicators, cervical segmental loading, and local intervertebral rotational risk still

require further investigation.

In this study, a coupled automotive seat finite element model and THUMS AM50 human body model were used to establish rear-impact simulation cases under seat angles of 0 °, 45 °, 90 °, and 135 °. By comparing neck injury indicators, cervical segmental N_{km}, IV-NIC_{rot}, cervical von Mises stress, and head injury responses, this study investigates the influence of seat angle variation on occupant head–neck injury mechanisms and provides a reference for rotating-seat protection design and non-standard posture safety assessment.

2. Methods

2.1. Coupled Seat–Occupant Finite Element Model

A coupled seat–occupant finite element model consisting of an automotive seat and the THUMS AM50 human body model [7] was established, as shown in Figure 1(a). The seat finite element model included the frame, slide rails, recliner, head restraint, foam padding, and other key components, which can represent the influence of seat support and deformation on occupant response during rear impact. The THUMS AM50 model represents a 50th percentile male biomechanical human body model and can describe the dynamic responses of the head, cervical spine, torso, and limbs.

Before the rear-impact simulations, the seat model was verified under a 20 g dynamic inertia condition and a 530 N·m seatback static strength condition, ensuring its structural reliability under impact loading.

To investigate the influence of seat rotation angle on occupant head–neck injury, four coupled models with different seat rotation angles were established. Except for the seat angle, the human body model, seat model, rear-impact acceleration pulse, restraint system, and contact definitions were kept consistent among all cases. In the model coordinate system, the vehicle forward direction was defined as the +Y axis, and the vertical upward direction was defined as the +Z axis. The seat rotation angle was defined as the rotation about the Z axis relative to the initial position along the +Y direction. The four angles were 0 °, 45 °, 90 °, and 135 °, rotating toward the +X direction, as shown in Figure 1(b).

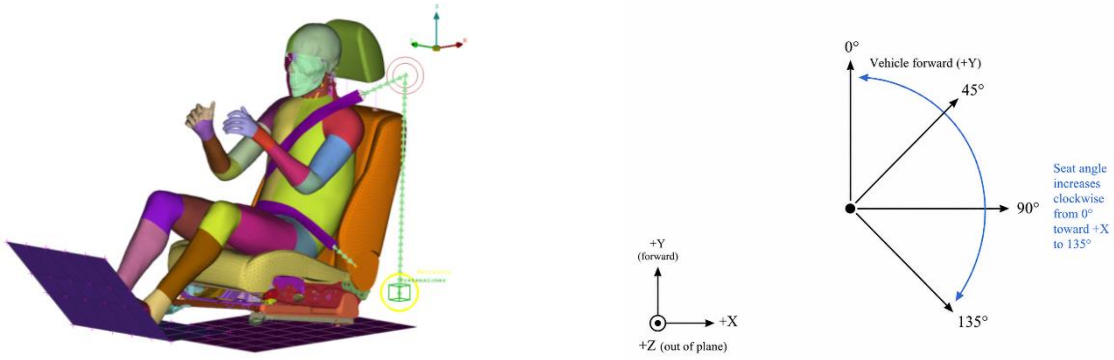

(a) (b)

Figure 1: Coupled seat-THUMS AM50 model and seat angle definition: (a) coupled seat-THUMS AM50 model; (b) seat angle definition.

2.2. Rear-Impact Simulation Cases

To systematically investigate the variation in occupant posture from a standard forward-facing posture to a large-angle rotated posture, four seat rotation cases were designed: 0 °, 45 °, 90 °, and 135 °. The 0 ° case represents the standard forward-facing posture and is used as the baseline case; the 45 ° case represents a slightly rotated posture; the 90 ° case represents a typical lateral rotated posture

facing the side window; and the 135 ° case represents a large-angle rotated posture. During the simulations, the bottom of the seat slide rails was constrained according to the vehicle installation condition, and a rear-impact acceleration pulse was applied to the coupled seat–occupant system, as shown in Figure 2.

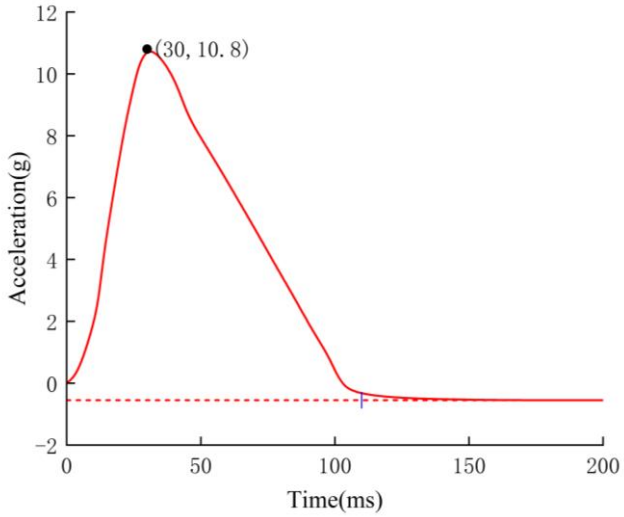

Figure 2: Rear-impact acceleration pulse.

As shown in Figure 2, the peak value of the rear-impact acceleration pulse is approximately 10.8 g, occurring at about 30 ms, and the main loading process lasts until approximately 110 ms. Except for the seat rotation angle, the human body model, seat model, restraint system, contact definitions, and loading conditions were kept consistent among the four cases to ensure comparability of the head–neck injury responses under different seat angles.

2.3. Injury Evaluation Indicators

Occupant injury was evaluated from four aspects: neck injury indicators, cervical segmental loading, local intervertebral rotational risk, and head injury response. The neck injury indicators included N_{km} and NIC. N_{km} reflects the combined injury risk associated with cervical shear force and bending moment [8], while NIC is used to evaluate the relative head–neck motion in rear impacts [6]. In addition, the peak N_{km} values of the C1–C7 cervical segments were extracted to analyze the variation in high-response cervical segments under different seat angles.

Considering that rotated seating postures may cause obvious asymmetric bending and local rotational responses of the cervical spine, IV-NIC_{rot} was introduced to evaluate intervertebral rotational risk. This indicator represents intervertebral rotational response based on the concept of IV-NIC and can supplement the local intervertebral rotational risk that is difficult to capture using N_{km} and NIC alone [9].

Head injury response was evaluated using BrIC and brain maximum principal strain. BrIC reflects the global rotational injury risk of the head, while brain maximum principal strain is used to characterize local tissue deformation risk [10-11].

3. Results and analysis

3.1. Overall Occupant Kinematic Response under Different Seat Angles

The overall kinematic response of the AM50 occupant differed clearly under different seat angles. In the 0 ° case, the occupant mainly exhibited a typical rearward whiplash motion, and the torso and

head–neck responses were relatively consistent in direction. In the 45 °case, the response still retained some features of a standard rear impact, but a lateral component began to appear in the head–neck motion. In the 90 ° case, the rear-impact loading direction formed a large angle with the initial occupant orientation, and the head–neck response changed from a single rearward motion to a coupled lateral deflection and rotational motion. In the 135 °case, the occupant posture change became more complex, with more evident head–neck deflection and local cervical response in the later stage.

Since the peak response time was not identical among different seat angles, typical postures were selected according to four response stages: initial posture, head restraint contact/response establishment, maximum head–neck response, and late-stage extreme posture. The corresponding postures are shown in Figure 3. As the seat angle increased, the head–neck motion gradually changed from a standard whiplash response to an asymmetric deflection and rotational coupling response, indicating that seat angle variation significantly changes the kinematic path and loading mode of the occupant head–neck complex during rear impact.

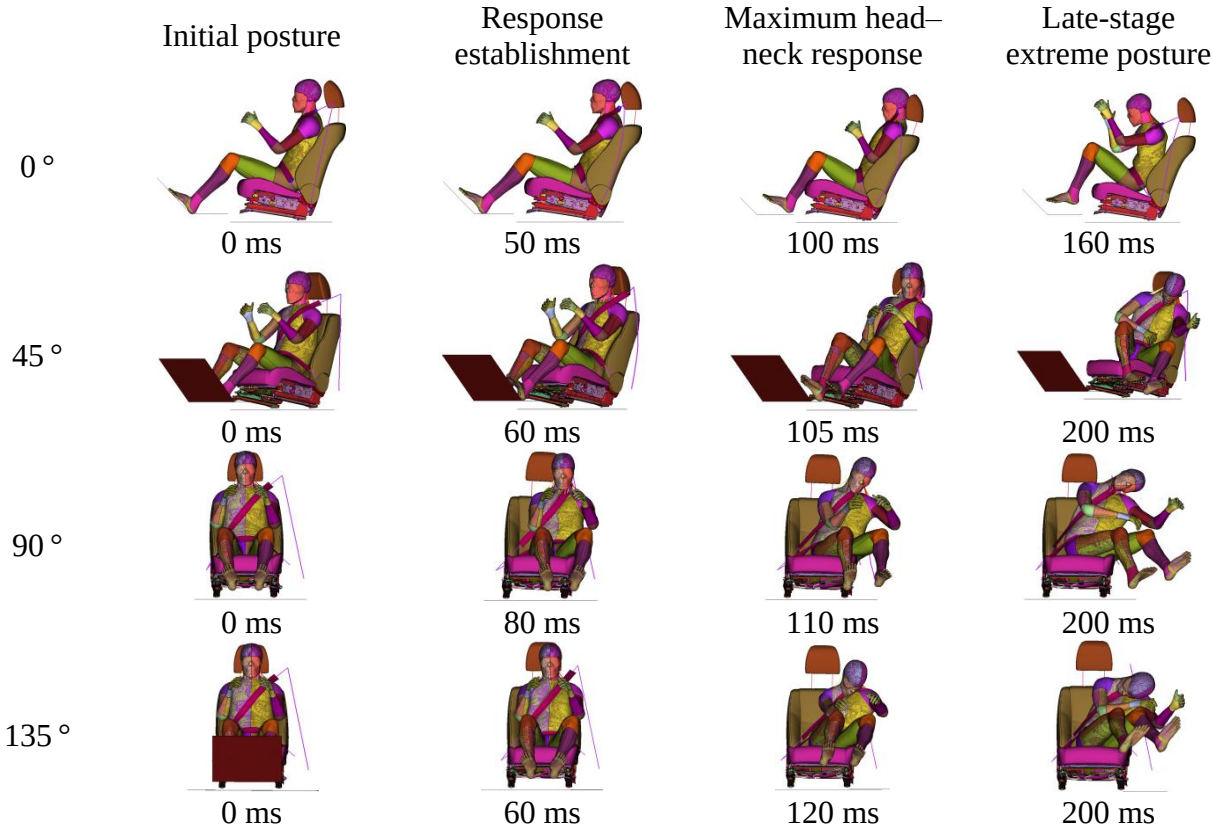

Figure 3: Key response‑stage postures of the AM50 occupant under different seat angles.

3.2. Neck Injury Responses under Different Seat Rotation Angles

3.2.1. Neck Injury Indicator Responses

The neck injury indicator responses of the AM50 occupant showed clear differences under different seat rotation angles. In the 0 °standard posture, the peak segmental N_{km} value was 0.069, occurring at the C2 segment, indicating an overall low response level. As the seat rotation angle increased, the peak segmental N_{km} gradually increased, reaching 0.143, 0.273, and 0.397 under the 45 °, 90 °, and 135 °cases, respectively. This indicates that rotated seating postures increase the local cervical shear–bending combined loading risk.

Meanwhile, the peak NIC increased from 14.60 m ⁄s ²in the 0 °case to 45.41 m ⁄s ², 46.97 m ⁄s ²,

and 49.33 m ⁄s ²in the 45 °, 90 °, and 135 °cases, respectively. This suggests that seat rotation enhances the velocity–acceleration coupling response of the head relative to T1. Therefore, seat rotation angle affects both local cervical loading and relative head–neck motion.

3.2.2. Cervical Segmental Nkm and IV-NICrot Responses

To further analyze the variation in cervical segmental loading under different seat angles, the peak N_{km} values of the C1–C7 segments were extracted, as shown in Table 1. In the 0 °standard posture, the N_{km} values of all segments were below 0.070, with the peak value occurring at C2. In the 45 °case, the segmental N_{km} values increased compared with the 0 °case, with the peak occurring at C4. In the 90 ° case, the responses at C2 and C6 increased significantly. In the 135 ° case, relatively high responses were observed at C1, C2, C6, and C7, with the C1 segment reaching 0.397, the highest value among all cases. These results indicate that, as the seat rotation angle increases, cervical segmental loading changes from a low-level response under the standard posture to a combined loading pattern involving both the upper and lower cervical spine.

Table 1: Peak Nkm values of cervical segments under different seat angles

Cervical segment	0 °	45 °	90 °	135 °
C1	0.058	0.140	0.223	0.397
C2	0.069	0.111	0.273	0.285
C3	0.045	0.088	0.129	0.156
C4	0.052	0.143	0.212	0.245
C5	0.041	0.100	0.138	0.147
C6	0.045	0.116	0.261	0.246
C7	0.054	0.110	0.102	0.280

Considering the asymmetric bending and local rotational characteristics of the cervical response after seat rotation, IV-NIC_{rot} was further used to evaluate the local intervertebral rotational risk under different seat angles, as shown in Table 2.

Table 2: IV-NICrot distribution of intervertebral segments under different seat angles

Intervertebral segment	0 °	45 °	90 °	135 °
C1–C2	0.49	0.53	0.49	0.65
C2–C3	0.59	0.96	0.53	1.18
C3–C4	0.69	1.00	0.97	0.92
C4–C5	0.66	1.29	0.63	0.67
C5–C6	0.68	1.89	0.74	0.76
C6–C7	0.73	1.32	0.61	1.58
C7–T1	0.93	1.17	0.57	3.76

As shown in Table 2, the IV-NIC_{rot} values in the 0 °standard posture were generally low, with the maximum value of 0.93 occurring at C7–T1. In the 45 °case, the IV-NIC_{rot} value at C5–C6 reached 1.89, indicating that local rotational risk may already appear in the middle-lower cervical spine under a slightly rotated posture. In the 90 °case, the IV-NIC_{rot} values were generally low, with a maximum value of 0.97. In the 135 °case, the IV-NIC_{rot} value at C7–T1 reached 3.76, much higher than that of the other cases and segments, indicating a prominent local rotational risk at the cervicothoracic junction. This result suggests that IV-NIC_{rot} can serve as a supplementary indicator to N_{km} and NIC for identifying local intervertebral rotational risk under different seat angles.

3.2.3. Cervical von Mises Stress Response

To further explain the migration of cervical risk under different seat angles from the perspective of local stress distribution, the von Mises stress distributions of the C1–C7 cervical segments were extracted for the AM50 occupant under the 0 °, 45 °, 90 °, and 135 ° cases, as shown in Figure 4. To ensure comparability among different cases, the same color scale range was used in Figure 4.

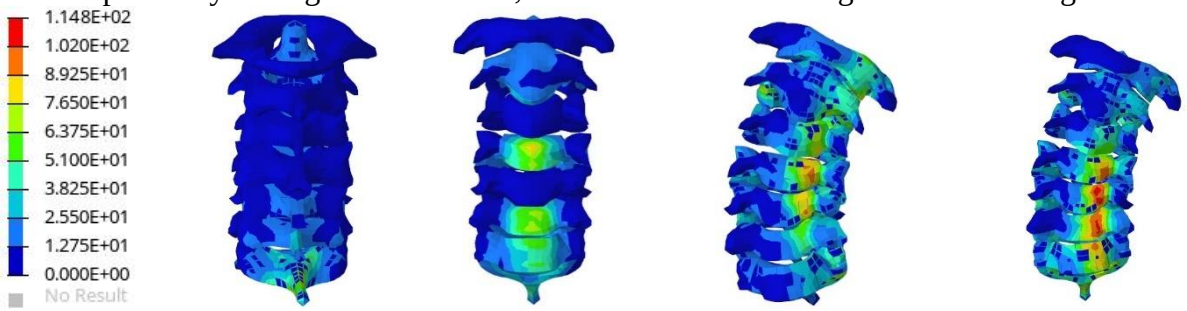

Figure 4: Von Mises stress distribution of the C1–C7 cervical segments of the AM50 occupant under different seat angles: (a) 0 ° case; (b) 45 ° case; (c) 90 ° case; (d) 135 ° case.

As shown in Figure 4, the cervical von Mises stress distribution in the 0 ° standard posture was relatively low, and the high-stress region was limited. In the 45 ° case, the local cervical stress increased, and the high-stress region began to concentrate in the middle-lower cervical spine. In the 90 ° case, the peak stress increased further, and the high-stress region gradually changed from a localized concentration to a continuous distribution in the middle-lower cervical spine. In the 135 ° case, the high-stress region became more evident and extended toward the middle-lower and terminal cervical segments. Combined with the peak cervical stresses of 89.1 MPa, 112.2 MPa, and 114.8 MPa under the 45 °, 90 °, and 135 ° cases, respectively, these results indicate that increasing seat angle enhances the local loading level of the cervical spine. This result is consistent with the segmental N_{km} and IV-NIC_{rot} results, indicating that the middle-lower cervical spine and cervicothoracic junction are more likely to become potential high-risk regions under large-angle rotated postures.

3.3. Head and Brain Tissue Injury Responses under Different Seat Angles

Based on the neck injury response analysis, the head rotational injury indicator and brain tissue deformation response of the AM50 occupant were further compared under different seat angles, as shown in Figure 5. In the 0 ° case, BrIC was 0.29 and brain maximum principal strain was 15.8%, both of which were lower than those in the three rotated cases. In the 45 °, 90 °, and 135 ° cases, the BrIC values were 0.83, 0.73, and 0.98, respectively, and the brain maximum principal strain values were 19.4%, 17.6%, and 24.4%, respectively. The 135 ° case produced the highest BrIC and brain maximum principal strain, indicating that large-angle seat rotation increases head rotational motion and local brain deformation risk.

It is worth noting that both BrIC and brain maximum principal strain in the 45 ° case were higher than those in the 90 ° case, indicating that the head injury response does not increase monotonically with seat angle. Instead, it is jointly affected by the initial occupant posture, head rotation direction, head restraint contact timing, and torso support condition. Overall, seat rotation increases the risk of head rotational injury and brain tissue deformation in rear impact, and the 135 ° large-angle rotated case should be considered a key condition.

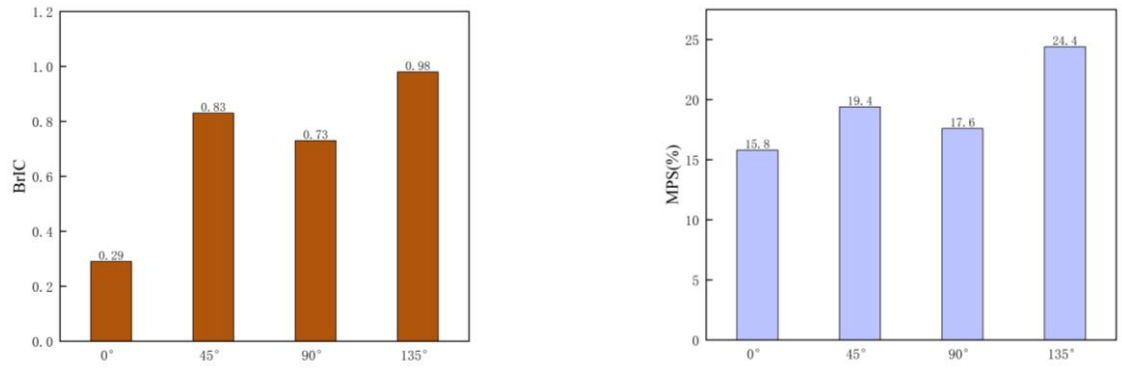

(a) (b)

Figure 5: Comparison of head injury indicators and brain tissue strain of the AM50 occupant under different seat angles: (a) BrIC; (b) brain maximum principal strain.

4. Discussion

The results show that seat angle variation clearly changes the head–neck injury response of the AM50 occupant in rear impact. In the 0 ° standard posture, the occupant mainly exhibits a typical whiplash motion, and the cervical segmental N_{km}, IV-NIC_{rot}, NIC, BrIC, and brain maximum principal strain are generally low. In the 45 °, 90 °, and 135 ° seat rotation cases, the initial occupant orientation forms an angle with the rear-impact loading direction, and the head–neck motion gradually shows lateral deflection and rotational coupling. As a result, cervical local loading, intervertebral rotational response, relative head–neck motion, and brain tissue deformation are enhanced.

For neck injury response, segmental N_{km}, NIC, and IV-NIC_{rot} describe different aspects of cervical risk. The peak segmental N_{km} increases with seat angle, while NIC is clearly higher in the rotated cases than in the 0 ° case. IV-NIC_{rot} further shows that the local rotational risk at C7–T1 is most prominent in the 135 ° case. The cervical von Mises stress contours also indicate that the high-stress region gradually extends toward the middle-lower and terminal cervical segments under rotated postures. These results suggest that large-angle seat rotation may cause both increased neck response and local segmental risk concentration.

For head and brain tissue responses, BrIC and brain maximum principal strain are higher in the rotated cases than in the 0 ° case, indicating increased head rotational motion and brain tissue deformation risk. However, the head injury response does not increase monotonically with seat angle, suggesting that it is jointly affected by occupant posture, head rotation direction, head restraint contact timing, and torso support condition. Therefore, rear-impact safety assessment for rotating seats should comprehensively consider occupant kinematics, cervical segmental loading, intervertebral rotation, cervical stress distribution, and head injury response.

This study still has limitations. Only the THUMS AM50 model was used, and differences among occupant body sizes were not considered. In addition, only four typical seat angles were selected, and the results were mainly obtained from finite element simulations. Future studies should include more occupant models, continuous seat angle variations, and experimental validation.

5. Conclusions

Based on the coupled seat–THUMS AM50 finite element model, rear-impact simulation cases under seat angles of 0 °, 45 °, 90 °, and 135 ° were established to analyze the influence of seat rotation

angle on the head–neck injury responses of a 50th percentile male occupant. The main conclusions are as follows.

First, seat angle variation changes the overall occupant kinematic response. In the 0 ° case, the occupant mainly exhibits a typical whiplash motion. As the seat angle increases, the head–neck motion gradually changes to coupled lateral deflection and rotational response.

Second, seat rotation enhances the neck injury response. In the 0 °case, the peak segmental N_{km} is 0.069, and it increases to 0.143, 0.273, and 0.397 in the 45 °, 90 °, and 135 ° cases, respectively. The peak NIC also increases from 14.60 m²/s² to 49.33 m²/s², indicating that rotated postures enhance cervical local loading and relative head–neck motion.

Third, local cervical risk becomes more prominent under large-angle rotation. In the 135 ° case, IV-NIC_{rot} reaches 3.76 at the C7–T1 segment, and the high-value region of cervical von Mises stress also extends toward the middle-lower and terminal cervical segments. This suggests that the cervicothoracic junction is a key risk region under large-angle rotated postures.

Fourth, the risk of head and brain tissue injury increases under rotated cases. BrIC and brain maximum principal strain are higher in the 45 °, 90 °, and 135 ° cases than in the 0 ° case, with the highest values appearing in the 135 °case. This indicates that large-angle seat rotation increases head rotational motion and local brain tissue deformation risk.

Overall, rear-impact injury assessment for rotating seats in intelligent driving scenarios should comprehensively consider overall kinematic response, cervical segmental loading, local intervertebral rotational risk, cervical stress distribution, and head injury response.

References

[1] SAE International. Taxonomy and definitions for terms related to driving automation systems for on-road motor vehicles: SAE J3016_202104[S]. Warrendale: SAE International, 2021.

[2] Jorlöv S, Bohman K, Larsson A. Seating positions and activities in highly automated cars: a qualitative study of future automated driving scenarios[C]//Proceedings of the IRCOBI Conference. Antwerp: IRCOBI, 2017: 13-22.

[3] Koppel S, Jimenez Octavio J, Bohman K, Logan D, Raphael W, Quintana Jimenez L, Lopez-Valdes F. Seating configuration and position preferences in fully automated vehicles[J]. Traffic Injury Prevention, 2019, 20(sup2): S103-S109.

[4] Östling M, Lubbe N, Jeppsson H, Puthan P. Passenger safety in future cars: a review of current human body models and injury criteria for seated occupants[J]. Traffic Injury Prevention, 2019, 20(sup2): S1-S7.

[5] Jakobsson L, Norin H, Svensson M Y. Parameters influencing AIS 1 neck injury outcome in vehicle rear impacts[J]. Traffic Injury Prevention, 2004, 5(2): 156-163.

[6] Boström O, Svensson M Y, Aldman B, et al. A new neck injury criterion candidate based on injury findings in the cervical spinal ganglia after experimental neck extension trauma[C]//Proceedings of the IRCOBI Conference. Dublin: IRCOBI, 1996: 123-136.

[7] Toyota Motor Corporation. Total Human Model for Safety: THUMS user manual[M]. Toyota: Toyota Motor Corporation, 2019.

[8] Schmitt K U, Muser M H, Niederer P, Walz F. Trauma biomechanics: an introduction to injury biomechanics[M]. Berlin: Springer, 2010.

[9] Panjabi M M, Ito S, Ivancic P C, Rubin W. Evaluation of the intervertebral neck injury criterion using simulated rear impacts[J]. Journal of Biomechanics, 2005, 38(8): 1694-1701.

[10] Takhounts E G, Craig M J, Moorhouse K, McFadden J, Hasija V. Development of brain injury criteria (BrIC)[J]. Stapp Car Crash Journal, 2013, 57: 243-266.

[11] Kleiven S. Predictors for traumatic brain injuries evaluated through accident reconstructions[J]. Stapp Car Crash Journal, 2007, 51: 81-114.